TITLE

Tumor regression after intravenous administration of targeted vesicles entrapping the vitamin E α-tocotrienol

AUTHOR NAMES AND AFFILIATIONS

Reatul Karim [a], Sukrut Somani [a], Majed Al Robaian [a], Margaret Mullin [b], Rumelo Amor [a], Gail McConnell [a], Christine Dufès [a, *]

[a] Strathclyde Institute of Pharmacy and Biomedical Sciences, University of Strathclyde, 161 Cathedral Street, Glasgow G4 0RE, United Kingdom

[b] College of Medical, Veterinary and Life Sciences, University of Glasgow, Glasgow G12 8QQ, United Kingdom

*** Corresponding author:** Christine Dufès
Strathclyde Institute of Pharmacy and Biomedical Sciences, University of Strathclyde, 161 Cathedral Street, Glasgow G4 0RE, United Kingdom
Phone: 44 -141 548 3796
Fax: 44 -141 552 2562
E-mail: C.Dufes@strath.ac.uk

ABSTRACT

The therapeutic potential of tocotrienol, a member of the vitamin E family of compounds with potent *in vitro* anti-cancer properties, is limited by its inability to specifically reach tumors following intravenous administration. The purpose of this study is to determine whether a novel tumor-targeted vesicular formulation of tocotrienol would suppress the growth of A431 epidermoid carcinoma and B16-F10 melanoma *in vitro* and *in vivo*.

In this work, we demonstrated that novel transferrin-bearing multilamellar vesicles entrapping α-T3 resulted in a dramatically improved (by at least 52-fold) therapeutic efficacy *in vitro* on A431 cell line, compared to the free drug. In addition, the intravenous administration of tocotrienol entrapped in transferrin-bearing vesicles resulted in tumor suppression for 30% of A431 and 60% of B16-F10 tumors, without visible toxicity. Mouse survival was enhanced by more than 13 days compared to controls administered with the drug solution only.

This tumor-targeted, tocotrienol-based nanomedicine therefore significantly improved the therapeutic response in cancer treatment.

KEYWORDS

Tocotrienol; transferrin; tumor targeting; delivery system; cancer therapy

1. Introduction

Tocotrienol, a member of the vitamin E family of compounds, is currently receiving increased attention because of its promising anti-tumor activity [1,2]. It has been reported to exert its anti-cancer effects through various mechanisms, such as activation of p53, modulation of Bax/Bcl-2 ratio, decrease of oxidative stress and induction of apoptosis [1-4]. It can also inhibit angiogenesis by downregulating the expression of the vascular endothelial growth factor (VEGF) receptor and blocking intracellular VEGF signaling. In addition, it is able to potentiate apoptosis through inhibition of DNA polymerase and telomerase and of NF-κB activation pathway [1-4]. This wide range of anti-cancer effects therefore makes tocotrienol a very promising therapeutic molecule.

However, its efficacy against cancer cells *in vivo* is hindered by its inability to specifically reach cancer cells at a therapeutic concentration, without affecting normal cells. Given its anti-proliferative properties, it is of the utmost importance to find a strategy to deliver this therapeutic drug specifically to its site of action.

On the basis that iron is essential for tumor cell growth and can be effectively carried to tumors by using transferrin receptors overexpressed on cancer cells [5,6], we recently demonstrated that the conjugation of transferrin (Tf) to vesicles entrapping tocotrienol-rich fraction (TRF) extracted from palm oil could lead to tumor regression, and even tumor suppression, on both the tested cancer cell lines, following intravenous injection to a murine model [7-9]. It resulted in complete tumor eradication for 50% of B16-F10 tumors and 20% of A431 tumors [7]. The treatments were well tolerated by the animals, without weight loss or apparent signs of toxicity.

These previous studies, however, used TRF but did not evaluate the anti-cancer potency of each individual tocotrienols and tocopherols forming TRF, which is a mixture of α, γ-, δ-tocotrienol, α-tocopherol and other tocotrienol-related compounds. Structurally, tocotrienols and tocopherols consist of a chroman ring linked to a phytyl side chain, which is saturated only for tocopherols. Furthermore, tocotrienols and tocopherols compounds differ in the number and position of methyl substituents attached to their chroman ring [10]. Hence, the therapeutic efficacy resulting from tocotrienol formulations could be further enhanced by entrapping only the most effective tocotrienol compound(s) within optimized tumor-targeted vesicles.

The objectives of this study are therefore 1) to evaluate the efficacy of the individual tocotrienols and tocopherols entrapped in transferrin-bearing vesicles against the *in vitro* viability of various cancer cells and 2) to optimize the delivery system carrying tocotrienol by a) increasing the amount of drug entrapped within the vesicles, b) optimizing the amount of transferrin grafted to the vesicles and c) optimizing the overall structure of the vesicles.

2. Materials and methods

2.1. Cell lines and reagents

α-tocotrienol (α-T3), γ-tocotrienol (γ-T3), δ-tocotrienol (δ-T3), α-tocopherol (α-Toc), human holo-transferrin, dimethylsuberimidate and all other chemicals that are not specifically mentioned below were purchased from Sigma Aldrich (Poole, UK). Solulan C24 came from Amerchol (Edison, NJ). D-α-tocopheryl polyethylene glycol 1000 succinate (TPGS) was obtained from Eastman Chemical Company (Kingsport, TN). A431 human epidermoid carcinoma and Bioware® B16-F10-luc-G5 mouse melanoma that expresses the firefly luciferase, were respectively purchased from the European Collection of Cell Cultures (Salisbury, UK) and Caliper Life Sciences (Hopkinton, MA). DMEM and RPMI-1640 cell culture media, fetal bovine serum, L-glutamine and penicillin-streptomycin were obtained from Invitrogen (Paisley, UK). Passive lysis buffer came from Promega (Southampton, UK).

2.2. Preparation and characterization of transferrin-bearing vesicles entrapping tocotrienol and tocopherol compounds

To prepare control vesicles entrapping tocotrienol (T3) and tocopherol (Toc), a mixture of Span 60 (65 mg), cholesterol (58 mg), Solulan C24 (54 mg) in a solution of either α-T3, γ-T3, δ-T3 or α-Toc (1 mg/mL, prepared in 0.2 mL dimethylsulfoxide and 1.8 mL glucose 5% solution) was shaken at 60 ^{o}C for 1 hour, before being probe sonicated with a Soniprep 150 (MSE, London, UK) for 4 min. Tf-bearing vesicles were then prepared by conjugating Tf (12 mg) to the control vesicles (2 mL), using dimethylsuberimidate as a cross-linker, as previously described [7-9]. Unentrapped T3 or Toc was removed by ultracentrifugation (150 000 g for 1h). The vesicle pellet was then resuspended in 2 ml glucose 5% solution.

Vesicles were visualized by transmission electron microscopy (TEM) on a LEO 912 energy filtering electron microscope (Zeiss, Jena, Germany), as previously described [11].

T3 and Toc entrapment in the vesicles was quantified by spectrofluorimetry using a Varian Cary Eclipse spectrofluorometer (Palo Alto, CA) following disruption of the vesicles with isopropanol. To do so, 50 µL of the vesicles prepared above were diluted 1:100 with isopropanol, before fluorescence intensity was measured using the respective λ_{ex} and λ_{em} of the compounds (λ_{ex}: 295 nm for α-T3 and α-Toc, 300 nm for γ-T3 and δ-T3; λ_{em}: 327 nm for α-T3, 330 nm for the 3 other compounds).

The amount of transferrin present on the surface of the vesicles was measured by Lowry assay [12].

Size and zeta potential of the vesicles were respectively determined by photon correlation spectroscopy and laser Doppler electrophoresis on a Zetasizer Nano-ZS (Malvern Instruments, Malvern, UK).

2.3. In vitro biological characterization

2.3.1. Cell culture

A431 and B16-F10-luc-G5 cell lines were respectively grown in DMEM or RPMI-1640 medium supplemented with 10% (v/v) fetal bovine serum, 1% (v/v) L-glutamine and 0.5% (v/v) penicillin-streptomycin. Cells were cultured at 37^{o}C in a humid atmosphere of 5% CO_2.

2.3.2. Efficacy against cancer cell viability

The efficacy of T3 and Toc entrapped in Tf-bearing vesicles, control vesicles or in solution against cancer cell viability was assessed in A431 and B16-F10 cell lines. Cells (2 x 10^3 cells per well in 96-well plates seeded 72 hours prior treatment) were incubated for 72 hours with T3/Toc formulations at final concentrations of 1.28 × 10^{-3} to 100 µg/mL drug. The activity of the formulations against cell viability was evaluated by measurement of the growth inhibitory concentration for 50% of the cell population (IC_{50}) in a standard MTT cell viability assay based on cellular metabolic activity (n=15).

2.3.3. Analysis of cellular uptake

Qualitative analysis of cellular uptake was performed by coherent anti-Stokes Raman scattering (CARS) microscopy. A431 cells were seeded in 4-well chamber slides at a concentration of 10^4 cells/ well. After 72 hours, they were incubated for 12 hours with α-T3 (0.2 µg/well), either entrapped in Tf-bearing vesicles, control vesicles or in solution. They were then washed three times with 1 mL PBS, fixed with 1 mL methanol for 10 minutes and finally washed 3 times with 1 mL distilled water before being examined with a home-made CARS microscope, as described before [13].

2.4. Optimization of the tocotrienol formulations

2.4.1. Combination therapy

To assess if the efficacy of T3 and Toc vesicles against cancer cell viability could be increased by co-entrapment of various T3 and Toc compounds, two Tf-bearing vesicular formulations containing all four components of TRF in various ratios were prepared. Formulations F25 and F75 contain respectively 25% and 75% of α-T3 while the other three components of TRF (γ-T3, δ-T3 and α-Toc) were distributed in equal percentages in the formulation (25% γ-T3, 25% δ-T3 and 25% α-Toc for F25, 8.33% γ-T3, 8.33% δ-T3 and 8.33% α-Toc for F75). Both formulations contain 1 mg/mL T3 and Toc compounds for a total volume of 2 mL. Vesicle size, zeta potential, percentage of drug loading and efficacy against A431 cancer cells viability were determined and compared between the formulations entrapping α-T3.

2.4.2. Drug loading

Three Tf-bearing vesicular formulations were prepared as described above, with respectively 4 mg, 6 mg and 8 mg α-T3 instead of 2 mg α-T3.

2.4.3. Amount of transferrin conjugated to the vesicles

Various amounts of Tf (respectively 6, 18, 24 and 30 mg of Tf, and 12, 36, 48 and 60 mg of dimethylsuberimidate) was conjugated on four formulations of vesicles loaded with 2 mg α-T3, prepared as described above.

2.4.4. Replacement of unilamellar vesicles by multilamellar vesicles

To evaluate if changes in the number of lipid bilayers forming the vesicles could increase the efficacy of T3 and Toc vesicles against cancer cell viability, new multilamellar vesicles entrapping α-T3 were prepared. α-T3 (2 mg) and TPGS (57 mg) in 2 mL distilled water were probe sonicated for 2 min, before being added to Span 60 (65 mg), cholesterol (58 mg) and dioleoyl phosphatidylethanolamine (DOPE) (6 mg). The resulting mixture was shaken at 60°C for 1 h and then probe sonicated for 4 min. Tf-bearing vesicles were prepared by conjugating 12 mg Tf to 2 mL vesicles as described above for unilamellar vesicles.

2.5. In vivo tumoricidal activity

All animal experiments conducted were approved by the local ethics committee and performed in accordance with the UK Home Office regulations. Female, immunodeficient BALB/c mice (initial mean weight 20 g) were housed in groups of five with a room temperature of 21 ± 2°C and alternating 12h light-dark cycle. A431 or B16-F10-luc-G5 cancer cells in exponential growth were subcutaneously implanted to both flanks of the mice (1×10^6 cells per flank). When tumors become palpable and reach a diameter of 5 mm, the mice (n=5) were intravenously injected with T3 encapsulated in Tf-bearing vesicles, control vesicles or in solution (10 µg T3 per injection) once daily for 20 days. The mice were observed daily for tumor growth and body weight. The tumor volume was determined by caliper measurements and calculated by the formula "volume = $d^3 \times \pi/6$".

Tumor growth was also monitored by bioluminescence imaging with an IVIS Spectrum (Caliper Life Sciences, Hopkinton, MA). Mice bearing subcutaneous B16-F10-luc-G5

tumors were treated intravenously as described above. Ten minutes prior to *in vivo* imaging, they received the luciferase substrate D-luciferin (150 mg/kg body weight) by intraperitoneal injection and were anaesthetized by isoflurane inhalation on Days 1, 3, 5 and 7. The light emitted from the bioluminescent tumors was detected for 2 min using Living Image® software and displayed as a pseudo-color overlay onto a gray scale animal image.

2.6. Statistical Analysis

Results were expressed as means ± standard error of the mean (S.E.M). Statistical significance was assessed by one-way analysis of variance (ANOVA) (to determine whether there are any statistically significant differences between the means of three or more independent groups), followed by Tukey multiple comparison post-test (Minitab® software, State College, PE) (to determine which means amongst a set of means differs from the rest). Differences were considered statistically significant for P values lower than 0.05.

3. Results

3.1. Preparation and characterization of transferrin-bearing vesicles entrapping tocotrienol and tocopherol compounds

Tf-bearing and control unilamellar vesicles entrapping tocotrienol compounds have been successfully prepared, as confirmed by TEM imaging (Fig. 1). These vesicles were able to entrap 69.9 ± 1.8 % of α-T3, 83.3 ± 3.0 % of γ-T3, 83.3 ± 2.0 % of δ-T3 and 68.9 ± 3.1 % of α-Toc. An amount of 10.1 ± 0.5 mg transferrin was conjugated to the vesicles, which corresponds to an increase compared to the conjugation of about 6 mg transferrin obtained in our previous studies [8]. As expected, the conjugation of Tf to the surface of the loaded vesicles resulted in a slightly larger z-average mean diameter of 133 nm (polydispersity: 0.20) than that of control vesicles (114 nm, polydispersity: 0.18). The grafting of Tf to the vesicles reduced their zeta potential compared to that of control vesicles (-30 mV and -25 mV respectively for Tf-bearing and control vesicles).

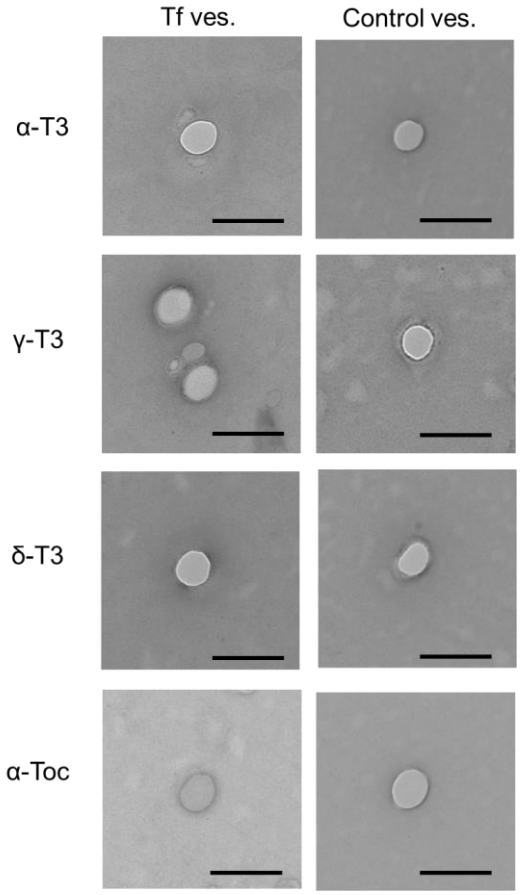

Figure 1. Transmission electron micrograph images of Tf-bearing and control unilamellar vesicles entrapping α-T3, γ-T3, δ-T3 and α-Toc (Bar: 200 nm).

3.2. In vitro efficacy against cancer cell viability

The *in vitro* efficacy against cancer cell viability of T3 and Toc compounds was significantly improved when formulated in Tf-bearing vesicles, by up to 1.6-fold on B16F10 cells and up to 1.7-fold on A431 cells when compared to control vesicles (Table 1). Among all the formulations tested, α-T3 and α-Toc entrapped in Tf-bearing vesicles resulted in the highest efficacy on B16F10 cells, with IC_{50} respectively of 1.07 ± 0.07 and 1.06 ± 0.18 µg/mL. In A431 cells, however, only α-T3 in Tf-bearing vesicles led to the highest efficacy against cancer cell viability, with an IC_{50} of 0.57 ± 0.26 µg/mL. Most of the tocotrienol

compounds formulated as solutions did not exert any effect on cell viability for the experimental parameters and concentrations used, probably due to their failure to be taken up by the cancer cells.

Table 1. Efficacy of α-T3, γ-T3, δ-T3 and α-Toc solutions against B16-F10 and A431 cancer cell viability, expressed as IC_{50} values (n=15)

B16F10 cells

Compound	IC_{50} (μg/mL) (mean ± S.E.M.)		
	Tf-vesicles	Control vesicles	Free drug
α-T3	1.07 ± 0.07	1.23 ± 0.19	50.48 ± 0.12
γ-T3	2.27 ± 0.39	2.97 ± 0.16	> 20
δ-T3	1.29 ± 0.11	1.39 ± 0.20	> 20
α-Toc	1.06 ± 0.18	1.71 ± 0.25	> 20

A431 cells

Compound	IC_{50} (μg/mL) (mean ± S.E.M.)		
	Tf-vesicles	Control vesicles	Free drug
α-T3	0.57 ± 0.26	0.99 ± 0.06	> 20
γ-T3	1.01 ± 0.15	1.33 ± 0.09	> 20
δ-T3	1.73 ± 0.52	2.94 ± 0.14	14.73 ± 0.20
α-Toc	1.13 ± 0.17	1.70 ± 0.48	> 20

3.3. Optimization of the tocotrienol formulation

3.3.1. Combination therapy

No significant changes in vesicle size or zeta potential were observed for Tf-bearing vesicles formulated as Formulations F25 and F75, which contain respectively 25% and 75% of α-T3 while the other three components of TRF γ-T3, δ-T3 and α-Toc were distributed in equal percentages in the formulation, compared to Tf-bearing vesicles entrapping 100% of α-T3 (Table 2A). These formulations have an average size ranging from 113 ± 1 nm to 115 ± 3 nm. Variations of the percentage of α-T3 entrapped in the formulation did not have an influence either on the charges of the vesicles (-32 ± 3 mV for F25, -29 ± 4 mV for F75, compared to -30 ± 2 mV for Tf-bearing vesicles entrapping 100% α-T3). However, F25 and F75 formulations showed a much higher percentage of drug loading compared to the formulation containing 100% α-T3 (respectively 74.4 ± 2.5%, 78.1 ± 0.5%, 69.9 ± 1.8% for F25, F75 and Tf-bearing vesicles entrapping 100% α-T3). This is possibly due to changes in overall lipophilicity, as F25 and F75 contains a mixture of T3 and Toc compounds. Despite this increase in drug loading, the formulation leading to the highest efficiency against A431 cell viability remained Tf-bearing vesicles entrapping 100% α-T3, which indicates that the presence of other compounds reduces the efficacy of α-T3 against cancer cell viability (Table 2A).

Table 2. Characteristics and efficacy of α-T3 entrapped in Tf-bearing vesicles optimized by variation of the following parameters, against A431 cancer cell viability (n=15):

A) variation of the percentage of α-T3 co-entrapped in Tf-bearing vesicles with other T3 and Toc compounds (Total amount of T3 and Toc per formulation: 2 mg)
B) variation of the amount of entrapped α-T3
C) variation of the amount of conjugated Tf to the vesicles
D) replacement of unilamellar vesicles by multilamellar vesicles

A

Percentage of α-T3	Average size (nm)	Zeta potential (mV)	Drug loading (%)	IC_{50} (μg/mL)
25%	115 ± 3	-32 ± 3	74.4 ± 2.5	1.21 ± 0.12
75%	113 ± 1	-29 ± 4	78.1 ± 0.5	1.27 ± 0.21
100%	114 ± 2	-30 ± 2	69.9 ± 1.8	0.57 ± 0.26

B

Amount of α-T3 (mg)	Drug loading (%)	Amount of entrapped drug (mg)	IC_{50} (μg/mL)
2	69.9 ± 1.8	1.40 ± 0.02	0.57 ± 0.26
4	63.5 ± 0.1	2.54 ± 0.01	3.50 ± 0.14
6	62.3 ± 0.6	3.74 ± 0.02	4.98 ± 0.33
8	71.7 ± 0.1	5.74 ± 0.01	5.06 ± 0.28

C

Amount of added Tf (mg)	Amount of conjugated Tf (mg)	Ligand conjugation (%)	IC_{50} (μg/mL)
6	5.2 ± 0.1	86.7 ± 2.3	0.95 ± 0.05
12	10.1 ± 0.5	84.2 ± 3.8	0.57 ± 0.26
18	15.0 ± 0.6	83.2 ± 3.6	0.92 ± 0.05
24	18.6 ± 0.4	77.3 ± 1.9	0.76 ± 0.03
30	19.3 ± 0.2	64.2 ± 0.6	0.80 ± 0.06

D

Type of vesicles	Average size (nm)	Zeta potential (mV)	Drug loading (%)	IC_{50} (μg/mL)
Tf-bearing MV	176 ± 1	-52 ± 3	69.9 ± 0.2	0.38 ± 0.07
Control MV	167 ± 1	-49 ± 2	69.2 ± 0.4	0.45 ± 0.06

3.3.2. Drug loading

The amount of α-T3 entrapped within Tf-bearing vesicles increased linearly with the increasing amounts of drug initially added to the formulations, ranging from 1.40 ± 0.02 mg to 5.74 ± 0.01 mg α-T3 (Table 2B). However, as the amount of entrapped α-T3 increased, the IC_{50} of the formulations also gradually increased from 0.57 ± 0.26 µg/mL until it reaches a plateau from 4.98 ± 0.33 µg/mL (Table 2B). This demonstrates that the amount of α-T3 within the bilayer vesicle membrane has a marked impact on the activity of the formulation against cancer cell viability.

3.3.3. Amount of transferrin conjugated to the vesicles

The amount of transferrin conjugated to the vesicles increased linearly with increasing amounts of transferrin added to the formulation (6 mg, 12 mg, 18 mg, 24 mg or 30 mg Tf), until it reached a plateau following addition of 24 mg transferrin, for which the vesicle surface became saturated with conjugated transferrin (18.6 ± 0.4 mg conjugated Tf) (Table 2C). Further increase in transferrin concentration marginally increased the amount of transferrin conjugated.

As transferrin was added in increasing amounts, the percentage of ligand conjugation decreased gradually (from 86.7 ± 2.3 % to 64.2 ± 0.6 % respectively for 6 mg Tf to 30 mg Tf added to the vesicles).

The IC_{50} values of all the formulations on A431 cells were below 1µg/mL (from 0.57 ± 0.26 µg/mL to 0.92 ± 0.05 µg/mL) and did not appear to follow a trend relative to the amount of conjugated Tf. The formulation to which 12 mg transferrin was initially added showed a significantly lowest IC_{50} value of 0.57 + 0.26 µg/mL.

3.3.4. Replacement of unilamellar vesicles by multilamellar vesicles

Multilamellar vesicles made of Span 60, cholesterol, TPGS and DOPE, and entrapping α-T3 were successfully prepared, as confirmed by TEM imaging (Fig. 2). The size of the multilamellar vesicles was significantly larger compared to that of Solulan C24-based unilamellar vesicles, with Tf-bearing vesicles being larger than control vesicles (respectively 176 ± 1 nm and 167 ± 1 nm for Tf-bearing and control vesicles) (Table 2D). Both Tf- and control vesicles were shown to be negatively charged, with zeta potentials of -52 ± 3 mV and -49 ± 2 mV respectively for Tf-bearing and control vesicles.

The percentage of drug loading was 69.9 ± 0.2 %, similar to what observed with the unilamellar vesicles. However, the IC_{50} for these formulations was significantly much lower than with unilamellar vesicles (respectively 0.38 ± 0.07 µg/mL and 0.45 ± 0.06 µg/mL for Tf-bearing and control vesicles).

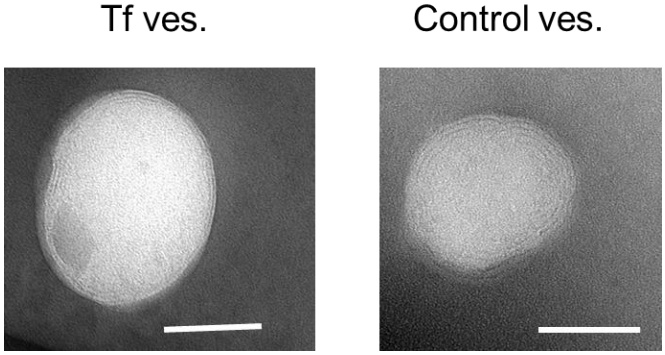

Figure 2. Transmission electron micrograph images of Tf-bearing and control multilamellar vesicles entrapping α-T3 (Bar: 100 nm).

3.4. Analysis of cellular uptake

The cellular uptake of α-T3 after treatment with Tf-bearing multilamellar vesicles was increased compared to control vesicles and the drug solution on A431 cell line (Fig. 3). In terms of intracellular distribution, CARS experiments showed that α-T3 was disseminated within the nucleus and cytoplasm of A431 cells following administration of Tf-bearing vesicles. By contrast, α-T3 administered in control vesicles or as a solution could not be detected. This might be explained by the threshold of the technique that probably allowed only the most intense CARS signals to be analyzed.

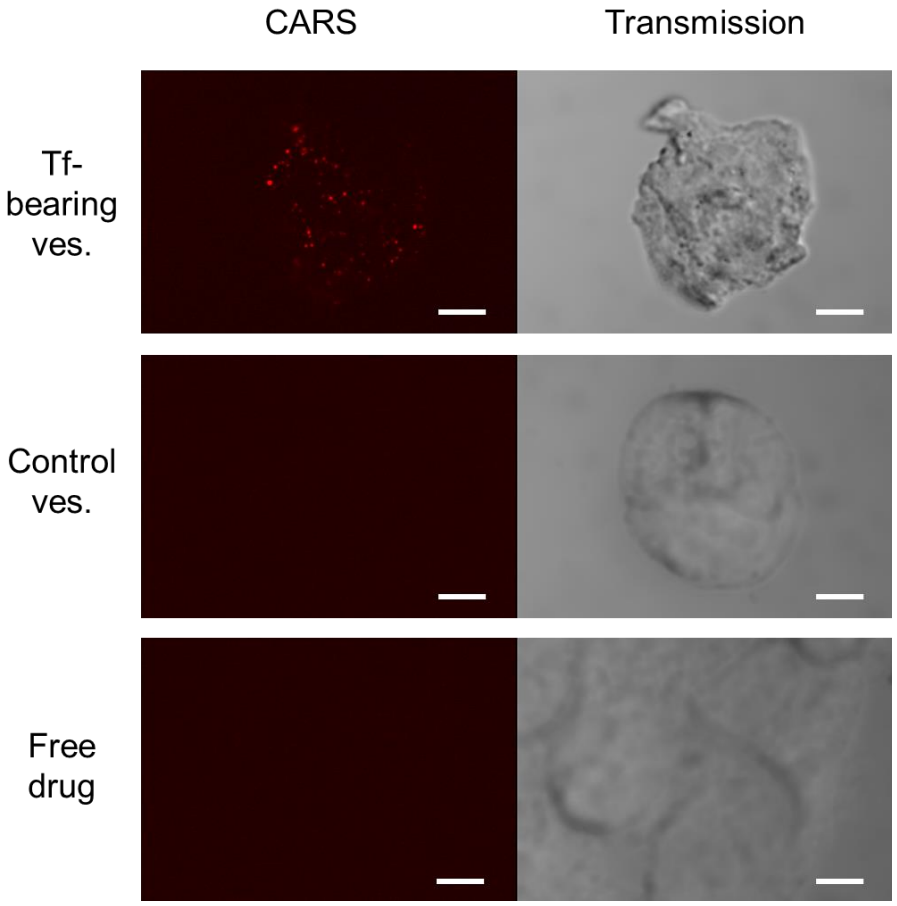

Figure 3. CARS and transmission microscopy imaging of the cellular uptake of α-T3 (0.2 μg/well) either entrapped in Tf-vesicles, control vesicles or in solution, after incubation for 12 hours in A431 cells. All images were taken in the size of 512 pixels x 512 pixels and with no averaging, at a frame capture rate of 1.68 s. The pump wavelength and the Stokes beam wavelength were tuned to 752.1 nm and 963.4 nm, corresponding to a Raman shift of 2916 cm^{-1} where the drug was expected to give the strongest CARS signals (bar: 50 μm).

3.5. In vivo tumoricidal activity

Intravenously administered α-T3 entrapped in Tf-bearing multilamellar vesicles led to tumor regression occurring within 24 hours on A431 tumors (Fig. 4A). This effect was maintained for 11 days, allowing the majority of the tumors to reach a size about half their initial size. From Day 11, while some tumors kept regressing, others started growing, which led to an overall slowdown of A431 tumor growth compared to the tumor growth observed with the other treatments. From Day 16, the mice bearing growing tumors reaching the maximum allowed size (13 mm) had to be euthanized. The other animals bearing smaller tumors were kept in the study. By contrast, none of the other treatments resulted in any A431 tumor regression.

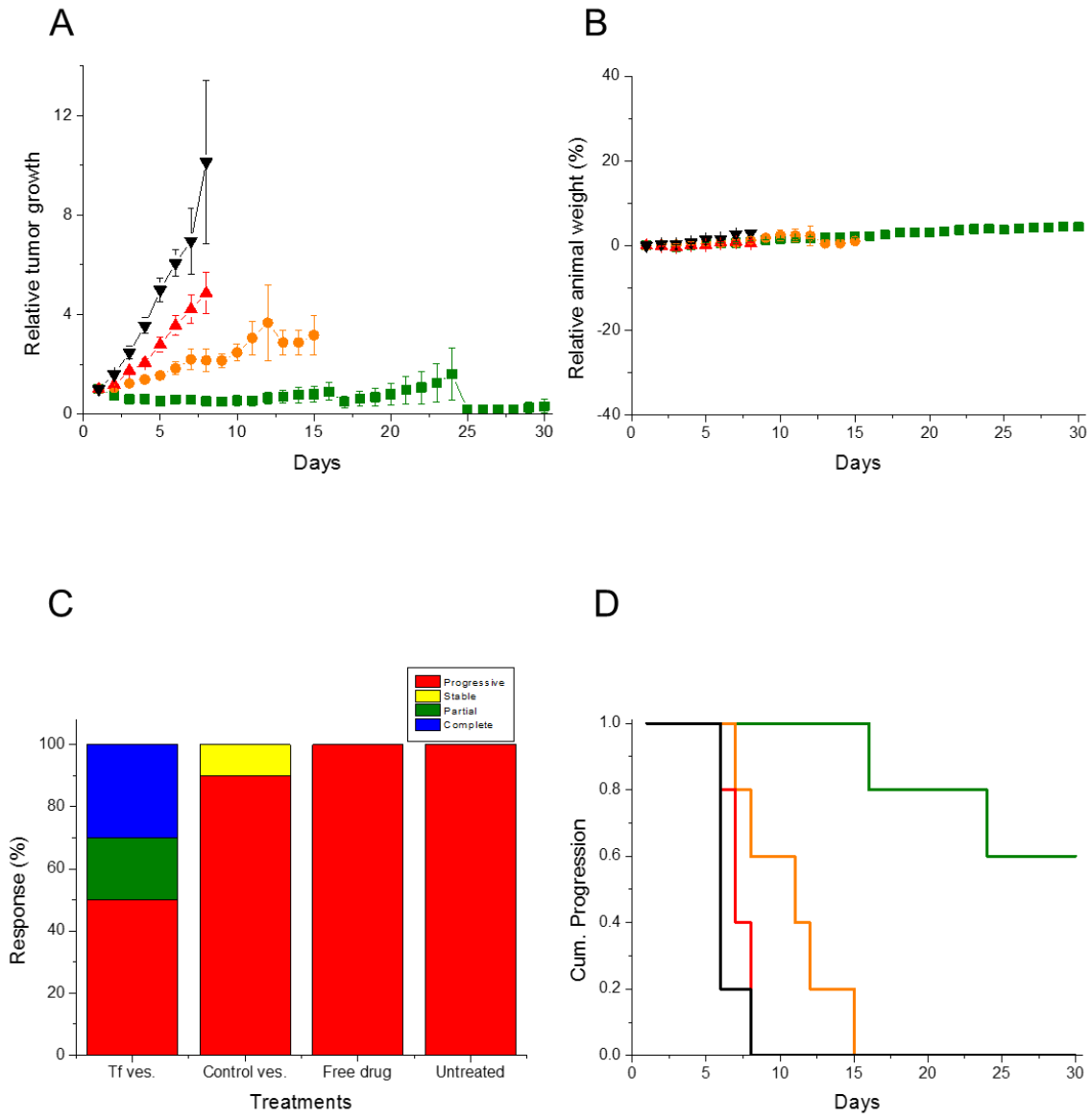

Figure 4. A) Tumor growth studies in a mouse A431 xenograft model after intravenous administration of Tf-bearing vesicles entrapping α-T3 (10 µg/injection) (green). Controls: control vesicles entrapping α-T3 (orange), α-T3 solution (red), untreated tumors (black) (n=10).
B) Variations of the animal body weight throughout the treatment (Color coding as in A).
C) Overall tumor response to treatments at the end of the study (Day 30).
D) Time to disease progression. The Y axis gives the proportion of surviving animals over time (Color coding as in A).

A similar pattern of tumor growth was observed as well on B16-F10-luc cells. α-T3 entrapped in intravenously administered Tf-bearing vesicles also led to tumor regression, but only for the first 3 days of the experiment (Fig. 5A). From Day 3, the treatment slowed growth overall compared to the other treatments, where tumor growth proceeded unchecked. From Day 14, the mice bearing tumors reaching the maximum allowed size (13 mm) had to be euthanized, while the others remained in the study. For this cell line as well, none of the other treatments resulted in tumor regression.

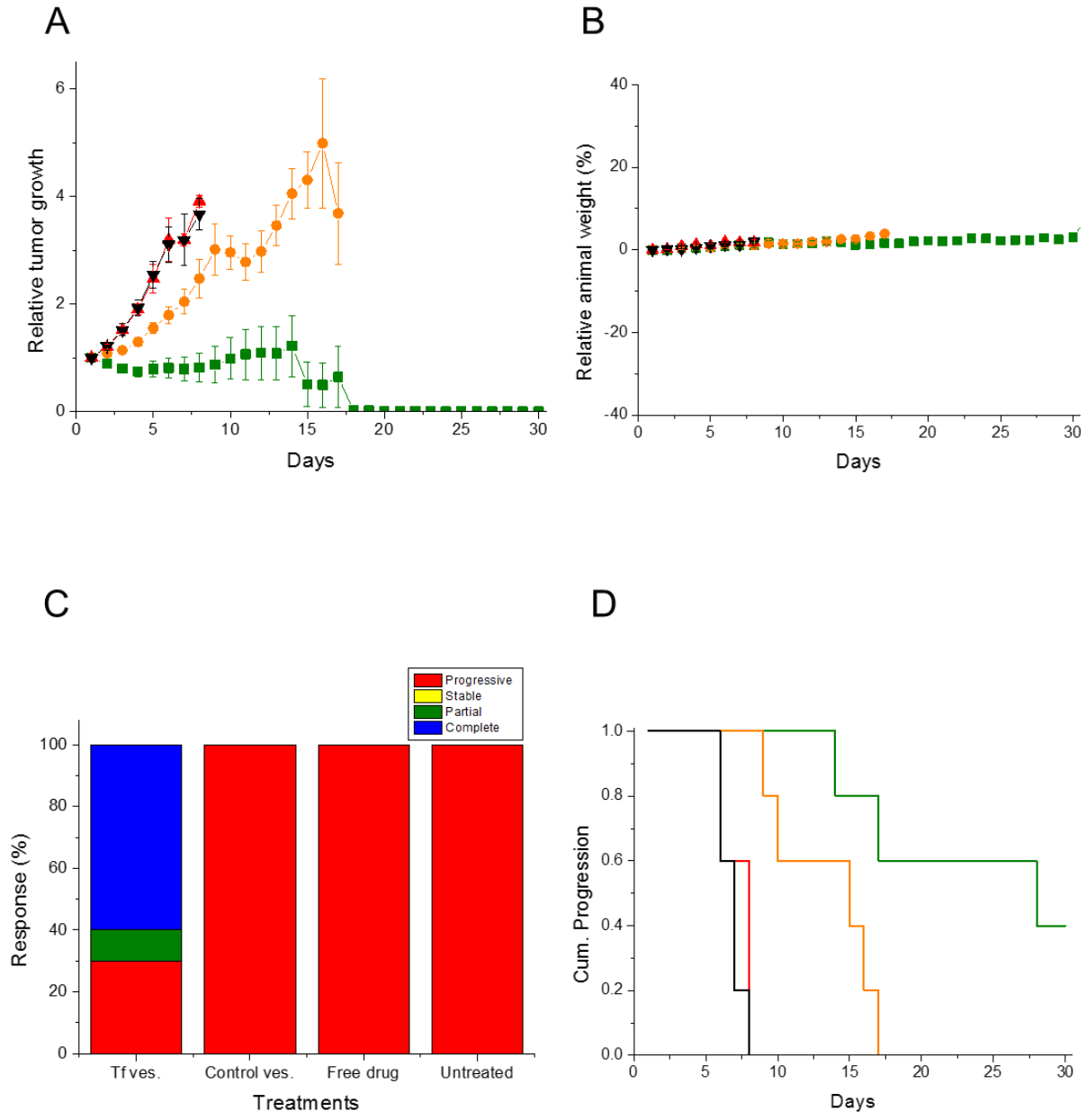

Figure 5. A) Tumor growth studies in a mouse B16-F10 xenograft model after intravenous administration of Tf-bearing vesicles entrapping α-T3 (10 µg/injection) (green). Controls: control vesicles entrapping α-T3 (orange), α-T3 solution (red), untreated tumors (black) (n=10).
B) Variations of the animal body weight throughout the treatment (Color coding as in A).
C) Overall tumor response to treatments at the end of the study (Day 30).
D) Time to disease progression. The Y axis gives the proportion of surviving animals over time (Color coding as in A).

The therapeutic effect resulting from treatment with α-T3 entrapped in Tf-bearing multilamellar vesicles was also qualitatively confirmed by bioluminescence imaging (Fig**.** 6). Following treatment with the Tf-bearing formulation, luciferase expression in the tumors gradually decreased from Day 1 to Day 7, whereas all the other treatments resulted in tumor growth.
All the treatments were well tolerated by the mice, and no apparent signs of toxicity or weight loss were observed (Fig**.** 4B and Fig. 5B).
On the last day of the experiment, 30% of A431 tumors and 60% of B16-F10-luc tumors treated with Tf-vesicles entrapping α-T3 had completely disappeared, while 20% of A431 tumors and 10% of B16-F10 tumors showed a partial response (Fig**.** 4C and Fig. 5C). In addition, 10% of A431 tumors were stable following treatment with control vesicles. However, 100% of the tumors treated with α-T3 solution or left untreated were progressive for both tumor types.
As a consequence of this enhanced therapeutic effect, animal survival was extended by 13 and 15 days respectively for mice bearing A431 and B16-F10 tumors, compared to untreated mice (Fig**.** 4D and Fig. 5D). The injection of control vesicles also increased the survival of the treated mice by 7 and 9 days respectively for A431 and B16-F10 tumors, compared to untreated animals.

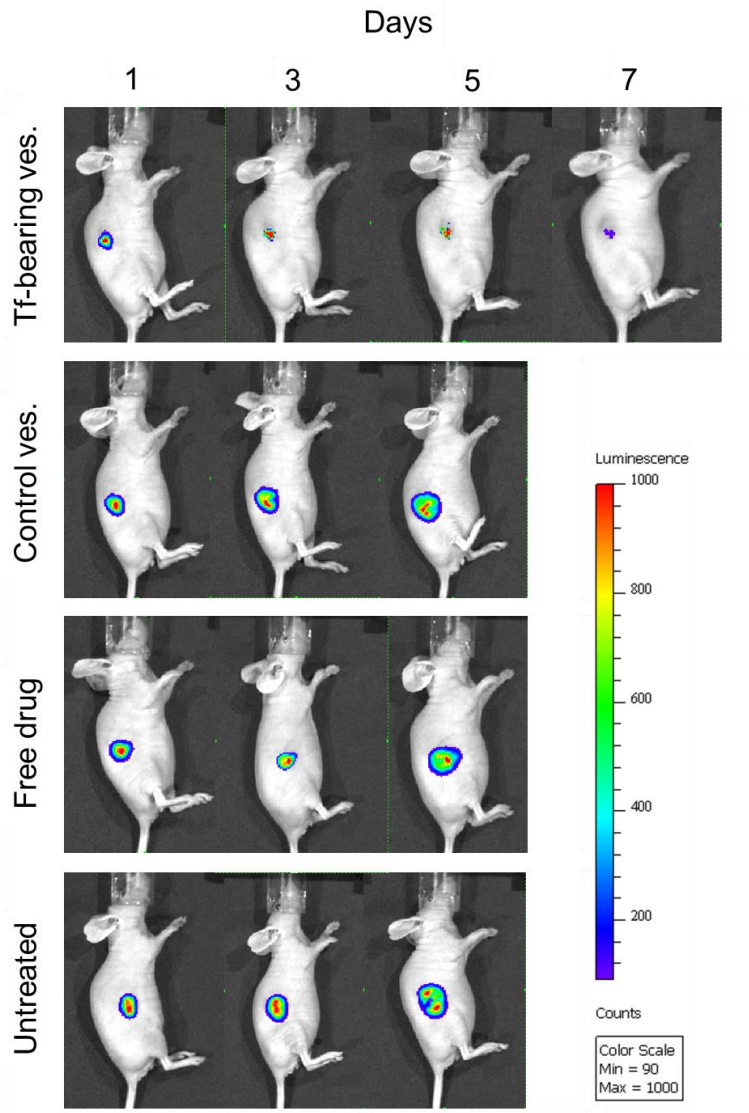

Figure 6. Bioluminescence imaging of the tumoricidal activity of α-T3 entrapped in Tf-bearing vesicles in a mouse B16-F10-luc tumor model. Controls: control vesicles entrapping α-T3, free α-T3 drug in solution, untreated tumors. The scale indicates surface radiance (photons/s/cm^2/steradian).

4. Discussion

The use of the vitamin E tocotrienol for the treatment of cancer has so far been limited by the inability of this drug to specifically reach tumors following systemic injection. To overcome this issue, we hypothesized that entrapping only the most efficacious tocotrienol compound(s) within a tumor-targeted delivery system that has been optimized to enhance the anti-proliferative effect of the carried drug, would increase the therapeutic efficacy *in vivo*.

Transferrin receptor is an attractive target for selective receptor-mediated drug delivery to tumors because of its overexpression on cancer cells, and has been widely used for tumor-targeted drug delivery [5,14]. In addition, the combination of transferrin-based active targeting with the passive targeting resulting from the enhanced permeability and retention effect [15] provides a tumor-selective targeting to this delivery system [16].

Among the various formulations investigated, multilamellar vesicles conjugated to 12 mg Tf and entrapping 2 mg of α-T3 were found to give the highest efficacy against A431 cell viability. These vesicles had a size lower than the cut-off size required for extravasation (which has been found to be 400 nm for most tumors [17,18]) and therefore have the required properties to access the transferrin receptor-expressing cancer cells and specifically deliver tocotrienol. In addition, their net negative charges would limit the risk of having electrostatic interactions between the vesicles and negatively charged cell membrane, therefore reducing any non-specific uptake of the vesicles by non-cancerous cells [19].

The entrapment of the lipophilic tocotrienol within the lipidic membranes of the vesicles offers the opportunity to administer this drug intravenously while shielding it from degradation, thus ensuring sufficient circulating tocotrienol available for reaching the tumors. Besides, multilamellar vesicles present the advantage of an increased drug loading and shielding from degradation, subsequently improving the dosing regimen and therapeutic index. In our previous study, transferrin-bearing, tocopheryl-based multilamellar vesicles entrapping tocotrienol rich fraction were shown to improve the drug uptake by A431 and B16-F10 cells [9], leading to an enhanced efficacy against cell viability *in vitro*. However, the IC_{50} obtained with this TRF-based formulation (0.89 ± 0.11 µg/mL on A431 cells, 4.09 ± 0.65 µg/mL on B16-F10 cells) were much higher than those obtained with our current α-T3–based formulation, highlighting the crucial need of entrapping only the most active member of the Vitamin E family in optimized vesicles. We could not find any other studies describing the anti-proliferative effect of tocotrienol entrapped in liposomes, unilamellar or multilamellar vesicles on cancer cells to allow a comparison with our results.

Among the various T3 and Toc compounds studied, α-T3 entrapped alone in Tf-bearing vesicles led to the highest efficacy against cancer cell viability. This result was unexpected, as α-T3 was often reported to be the least potent pro-apoptotic inducer in the literature, when compared to all the other tocotrienols [20]. Individual tocotrienols and tocopherols display differential potencies in suppressing tumor cell growth and inducing apoptosis depending of the cell lines studied. For example, α-T3 and γ-T3 were shown to effectively suppress the development of sarcoma 180, Ehrlich carcinoma and invasive mammary carcinoma [21]. However, in DLD-1 human colorectal adenocarcinoma and HepG2 human hepatoma cells, α-T3 was the least effective among all T3 compounds [22]. Similarly, in another study, γ- and δ-T3 reduced cell viability on SKBR3 and MCF-7 breast cancer cell lines with IC_{50} values of less than half those of α-T3 [23]. α-T3 also exhibited the least potent cytotoxicity towards both A549 and U87MG cells compared to δ-T3 and γ-T3 [23]. However, the IC_{50} reported in these publications were obtained following treatment with α-T3 solution, and were much higher than those obtained in our study with α-T3 entrapped in targeted vesicles, thus demonstrating the need of a targeted delivery system to capture the full potential of the tocotrienol compound against cell viability.

The presence of the lipophilic drug α-T3 within the bilayer structure may influence the membrane characteristics of the vesicle. As the amount of entrapped α-T3 increased, the

IC_{50} of the formulations increased gradually until it reached a plateau. This unexpected result indicates that changes in the amount of α-T3 entrapped within the bilayer vesicle membrane have a marked impact on the *in vitro* activity of the formulation against cell viability by modifying physicochemical characteristics that may have altered its cellular permeability, uptake and efficacy.

The IC_{50} values changed in irregular fashion with respect to the conjugated amount of transferrin or amount of entrapped drug. However, it is interesting to note that the formulation with the highest drug entrapment efficacy also resulted in the lowest IC_{50} value in A431 cell line, although formulations with higher amounts of transferrin were assessed. These results indicate that obtaining an optimum amount of transferrin conjugation and an optimum drug entrapment within the vesicles is a major factor to enhance the activity of the formulation against cancer cell viability.

Cellular uptake studies demonstrated that the conjugation of Tf to the vesicles significantly increased α-T3 uptake by A431 cells, compared with control vesicles and tocotrienol solution. These results were in agreement with our previous experiments that showed that the presence of Tf on similar vesicles enhanced the uptake of TRF by at least 1.5-fold for the same cell line [9].

In vivo, we demonstrated that the intravenous administration of α-T3 entrapped within Tf-bearing vesicles resulted in complete tumor eradication for 30% of A431 and 60% of B16-F10 tumors, and partial tumor regression for 20% of A431 cells and 10% of B16-F10 cells. This work corresponds to a major improvement of the therapeutic efficacy of this drug for the treatment of distant tumors. As far as we know, this work corresponds to the first preparation of a tumor-targeted delivery system able to entrap a single tocotrienol. Other researchers have previously demonstrated the ability of TRF co-entrapped with simvastatin in lipid nanoparticles to have an enhanced anti-proliferative effect against +SA mammary epithelial cancer cell line, in comparison with control α-tocopherol nanoparticles (with respective IC_{50} of 0.52 µM and 17.7 µM), but only *in vitro* and while using TRF rather than a tocotrienol compound [24]. The therapeutic effects observed in this current study were even more pronounced than those obtained in our previous studies with Tf-bearing multilamellar vesicles entrapping TRF, which resulted in tumor eradication of 20% of A431 tumors and 40% of B16-F10 tumors [9], and with Tf-bearing unilamellar vesicles entrapping TRF, which led to complete disappearance of 20% of A431 and 50% of B16-F10 cells [7]. This demonstrates the ability of α-T3 to exert an anti-cancer effect *in vivo* on the tested cancer cell lines, provided it is targeted to the tumors. Furthermore, this intravenously administered nanomedicine was able to act upon subcutaneously implanted tumors and should therefore have the potential to target metastatic tumors disseminated throughout the body.

5. Conclusions

In this study, we have demonstrated for the first time that a novel formulation of α-T3 entrapped in tumor-targeted vesicles can lead to complete tumor eradication for up to 60% of the tested tumors, following intravenous administration.

Among the various formulations investigated, multilamellar vesicles conjugated to 12 mg Tf and entrapping 2 mg of α-T3 were found to give the highest efficacy against A431 cancer cell viability *in vitro*.

In vivo, α-T3 entrapped in Tf- bearing multilamellar vesicles resulted in complete tumor suppression for 60% of B16-F10 tumors and 30% of A431 tumors, with long-term survival of the animals. By contrast, 100% of the tumors treated with the tocotrienol solution or left untreated were progressive for both tumor types. Animal survival was improved by more than 13 days compared to controls. The treatments were well tolerated by the animals. Transferrin-bearing vesicles entrapping α-T3 therefore hold great potential as a novel approach for cancer therapy.

ACKNOWLEDGMENTS
This work was financially supported by the University of Strathclyde.

REFERENCES
[1] D. Hussein, H. Mo, δ-tocotrienol-mediated suppression of the proliferation of human PANC-1, MIA PaCa-2, and BxPC-3 pancreatic carcinoma cells, Pancreas 38 (2009) 124-136.
[2] W.N. Yap, P.N. Chang, H.Y. Han, D.T. Lee, M.T. Ling, Y.C. Wong, Y.L. Yap, γ-tocotrienol suppresses prostate cancer cell proliferation and invasion through multiple-signalling pathways, Br. J. Cancer 99 (2008) 1832-1841.
[3] T. Miyazawa, A. Shibata, P. Sookwong, Y. Kawakami, T. Eitsuka, A. Asai, S. Oikawa, K. Nakagawa, Antiangiogenic and anticancer potential of unsaturated vitamin E (tocotrienol), J. Nutr. Biochem. 20 (2009) 79-86.
[4] K. Nesaretnam, Multitargeted therapy of cancer by tocotrienols, Cancer Lett. 269 (2008) 388-395.
[5] T.R. Daniels, T. Delgado, G. Helguera, M.L. Penichet, The transferrin receptor part II: targeted delivery of therapeutic agents into cancer cells, Clin. Immunol. 121 (2006) 159-176.
[6] A. Calzolari, I. Oliviero, S. Deaglio, G. Mariani, M. Biffoni, N.M. Sposi, F. Malavasi, C. Peschle, U. Testa, Transferrin receptor 2 is frequently expressed in human cancer cell lines, Blood Cells Mol. Dis. 39 (2007) 82-91.
[7] J.Y. Fu and C. Dufès, Anti-cancer efficacy of intravenously administered tumor-targeted vesicles entrapping tocotrienol, Pharm. Nanotechnology 22 (2014) 172-181.
[8] J.Y. Fu, D.R. Blatchford, L. Tetley, C. Dufès, Tumor regression after systemic administration of tocotrienol entrapped in tumor-targeted vesicles, J. Control. Release 140 (2009) 95-99.
[9] J.Y. Fu, W. Zhang, D.R. Blatchford, L. Tetley, G. McConnell, C. Dufès, Novel tocotrienol-entrapping vesicles can eradicate solid tumors after intravenous administration, J. Control. Release 154 (2011) 20-26.
[10] A. Kamal-Eldin, L.A. Appelqvist, The chemistry and anti-oxidant properties of tocopherols and tocotrienols, Lipids 31 (1996) 671-701.
[11] F. Lemarié, C.W. Chang, D.R. Blatchford, R. Amor, G. Norris, L. Tetley, G. McConnell, C. Dufès, Anti-tumor activity of the tea polyphenol epigallocatechin gallate encapsulated in targeted vesicles after intravenous administration, Nanomedicine 8 (2013) 181-192.
[12] O.H. Lowry, N.J. Rosenburgh, A.L. Farr, R.J. Randall, Protein measurement with the Folin phenol reagent, J. Biol. Chem. 193 (1951) 265–275.
[13] W. Zhang, M. Parsons, G. McConnell, Flexible and stable optical parametric oscillator based laser system for coherent anti-Stokes Raman scattering microscopy, Microsc. Res. Tech. 73 (2010) 650-656.
[14] F. Yuan, M. Dellian, D. Fukumura, M. Leunig, D.A. Berk, V.P. Torchilin, R.K. Jain, Vascular permeability in a human tumor xenograft: molecular size dependence and cutoff size, Cancer Res. 55 (1995) 3752-3756.
[15] O. Ishida, K. Maruyama, K. Sasaki, M. Iwatsuru, Size-dependent extravasation and interstitial localization of polyethyleneglycol liposomes in solid tumor-bearing mice, Int. J. Pharm. 193 (1999) 49-56.
[16] R. Kircheis, L. Wightman, A. Schreiber, B. Robitza, V. Rössler, M. Kursa, E. Wagner, Polyethylenimine/DNA complexes shielded by transferrin target gene expression to tumors after systemic application, Gene Ther. 8 (2001) 28-40.
[17] C. Dufès, M. Al Robaian, S. Somani, Transferrin and the transferrin receptor for the targeted delivery of therapeutic agents to the brain and cancer cells, Ther. Deliv. 4 (2013) 629-640.

[18] H. Maeda, The tumor blood vessel as an ideal target for macromolecular anticancer agents, J. Control. Release 19 (1992) 315-324.
[19] Z.M. Qian, H. Li, H. Sun, K. Ho, Targeted drug delivery via the transferrin receptor-mediated endocytosis pathway, Pharmacol. Rev. 54 (2002) 561-587.
[20] M. Sakai, M. Okabe, H. Tachibana, K. Yamada, Apoptosis induction by γ-tocotrienol in human hepatoma Hep3B cells, J. Nutr. Biochem. 17 (2006) 672-676.
[21] K. Komiyama, K. Iizuka, M. Yamaoka, H. Watanabe, N. Tsuchiya, I. Umezawa, Studies on the biological activity of tocotrienols, Chem. Pharm. Bull. 37 (1989) 369-371.
[22] A. Shibata, K. Nakagawa, P. Sookwong, T. Tsuduki, S. Tomita, H. Shirakawa, M. Komai, T. Miyazawa, Tocotrienol inhibits secretion of angiogenic factors from human colorectal adenocarcinoma cells by suppressing hypoxia-inducible factor-1α, J. Nutr. 138 (2008) 2136-2142.
[23] E. Pierpaoli, V. Viola, F. Pilolli, M. Piroddi, F. Galli, M. Provinciali, γ-and δ-tocotrienols exert a more potent anticancer effet than α-tocopheryl succinate on breast cancer cell lines irrespective of HER-2/neu expression, Life Sci. 86 (2010) 668-675.
[24] H. Ali, A.B. Shirode, P.W. Sylvester, S. Nazzal, Preparation, characterization and anticancer effects of simvastatin-tocotrienol lipid nanoparticles, Int. J. Pharm. 389 (2010) 223-231.